



# How does sodium sulfate crystallize? Implications for the decay and testing of building materials

Carlos Rodriguez-Navarro<sup>a,\*</sup>, Eric Doehne<sup>a</sup>, Eduardo Sebastian<sup>b</sup>

<sup>a</sup>The Getty Conservation Institute, 1200 Getty Center Drive, Suite 700, Los Angeles, CA 90049, USA

<sup>b</sup>Departamento de Mineralogía y Petrología, Universidad de Granada, c/Fuente Nueva s/n, Granada 18002, Spain

Received 29 June 1998; accepted 31 July 2000

## Abstract

The fundamental behavior of sodium sulfate crystallization and induced decay in concrete and other building materials is still poorly understood, resulting in some misinterpretation and controversy. We experimentally show that under real world conditions, both thenardite ( $\text{Na}_2\text{SO}_4$ ) and mirabilite ( $\text{Na}_2\text{SO}_4 \cdot 10\text{H}_2\text{O}$ ) precipitate directly from a saturated sodium sulfate solution at room temperature ( $20^\circ\text{C}$ ). With decreasing relative humidity (RH) and increasing evaporation rate, the relative proportion of thenardite increases, with thenardite being the most abundant phase when precipitation occurs at low RH in a porous material. However, thenardite is not expected to crystallize from a solution at  $T < 32.4^\circ\text{C}$  under equilibrium conditions. Non-equilibrium crystallization of thenardite at temperatures below  $32.4^\circ\text{C}$  occurs due to heterogeneous nucleation on a defect-rich support (i.e., most porous materials). Anhydrous sodium sulfate precipitation is promoted in micropores due to water activity reduction. Fast evaporation (due to low RH conditions) and the high degree of solution supersaturation reached in micropores before thenardite precipitation result in high crystallization pressure generation and greater damage to porous materials than mirabilite, which crystallizes at lower supersaturation ratios and generally as efflorescence. Data from the environmental scanning electron microscope (ESEM) show no hydration phenomena following wetting of thenardite; instead, thenardite dissolution occurs, followed by thenardite plus mirabilite crystallization upon drying. These results offer new insight into how damage is caused by sodium sulfate in natural geological, archaeological, construction and engineering contexts. They also help explain some of the controversial results of various commonly used sodium sulfate crystallization tests. © 2000 Elsevier Science Ltd. All rights reserved.

**Keywords:** Sodium sulfates; Humidity; SEM; X-ray diffraction; Degradation

## 1. Introduction

The crystallization of soluble salts in porous construction materials has been recognized as an important weathering process contributing to the decay of masonry, cement, and mortar in a range of environments [1,2]. In modern buildings, highways, and civil engineering works, salt weathering has been connected, in many cases, to the crystallization of soluble salts (e.g. sodium and calcium sulfates) released from Portland cement [3]. Among those salts, sodium sulfate has been found to be particularly damaging [4–6]. This latter salt is responsible for significant damage to porous building materials which are apparently caused by

the generation of high crystallization and hydration pressures [7–9]. Its destructive nature has made it the salt of choice to perform accelerated decay tests for estimating the durability of building materials (e.g. ASTM aggregate sound test [10], RILEM PEM/25 [11–13]).

However, the significance and the accuracy of sodium sulfate crystallization tests have been questioned [14,15]. Price [12] reported inconsistent results when comparing sodium sulfate crystallization test data from various laboratories using the same standard and materials. The controversy surrounding the various sodium sulfate crystallization tests has resulted in some researchers discouraging its use [15]. This situation seems to be exacerbated by a lack of a fundamental understanding of the sodium sulfate system and the crystallization of its various phases under real world conditions.

The  $\text{Na}_2\text{SO}_4\text{--H}_2\text{O}$  system (Fig. 1a and b) includes two stable phases [16–18]. Thenardite ( $\text{Na}_2\text{SO}_4$ ) is the anhy-

\* Corresponding author. Departamento de Mineralogía y Petrología, Universidad de Granada, c/Fuente Nueva s/n, Granada 18002, Spain. Tel.: +34-958-243-340; fax: +34-958-243-368.

E-mail address: carlosrn@ugr.es (C. Rodriguez-Navarro).

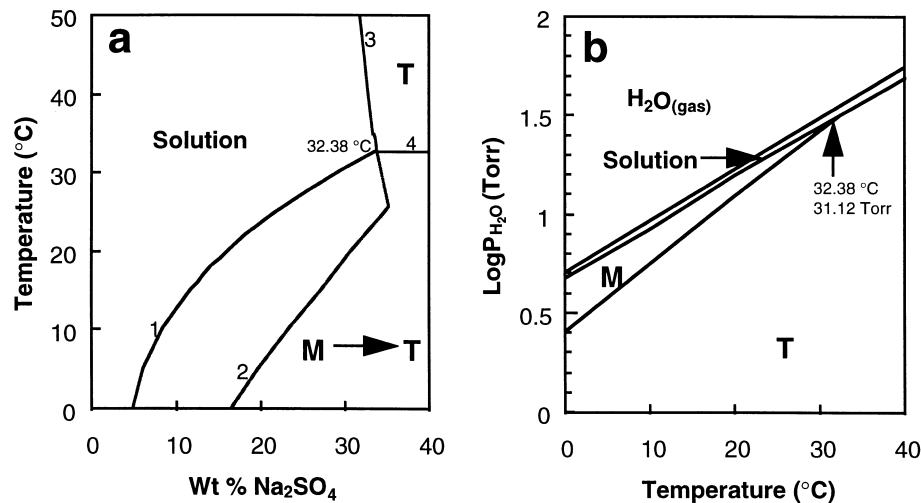


Fig. 1. The system,  $\text{Na}_2\text{SO}_4\text{-H}_2\text{O}$ . (a) Temperature vs. concentration diagram (M=mirabilite; T=thenardite; 1=solubility curve for  $\text{Na}_2\text{SO}_4\cdot 10\text{H}_2\text{O}$ ; 2=solubility curve for  $\text{Na}_2\text{SO}_4\cdot 7\text{H}_2\text{O}$ ; 3=solubility curve for  $\text{Na}_2\text{SO}_4$ ; 4= $\text{Na}_2\text{SO}_4/\text{Na}_2\text{SO}_4\cdot 10\text{H}_2\text{O}$  boundary). (b)  $P/T$  phase diagram for the system,  $\text{Na}_2\text{SO}_4\text{-H}_2\text{O}$ . Data sources: Refs. [16,19,20].

drous phase and is reported to precipitate directly from solution at temperatures above  $32.4^\circ\text{C}$  [19,21]. Below this temperature, the stable phase is mirabilite ( $\text{Na}_2\text{SO}_4\cdot 10\text{H}_2\text{O}$ ), which rapidly dehydrates at relative humidity (RH) below 71% ( $20^\circ\text{C}$ ) to form thenardite [21,22]. Thenardite will rehydrate to mirabilite if the humidity rises over 71%. Sodium sulfate heptahydrate ( $\text{Na}_2\text{SO}_4\cdot 7\text{H}_2\text{O}$ ) has been described as precipitating at temperatures below the mirabilite–thenardite transition point. However, this phase is metastable and has not been clearly identified in nature [17]. Sodium sulfate also undergoes various polymorphic transitions with temperature. At least five polymorphs of sodium sulfate (I, II, III, IV, and V) have been identified [23,24]. At room temperature ( $20^\circ\text{C}$ ), phase V is reported to be stable, while phase III is metastable at this condition [23]. Phases I and II are high-temperature polymorphs ( $>270^\circ\text{C}$  and  $>225^\circ\text{C}$ , respectively); however, phase II is reported to have a narrow stability zone [24]. Phase IV is considered to be metastable and its phase relation and structure have yet to be well established [24].

While many studies have investigated the crystallization and hydration of sodium sulfate, our understanding of the damage mechanism as well as the dynamics of this process is incomplete [25]. Many authors have ascribed the damage caused by this salt to the volume change and hydration pressure generated when thenardite is transformed to mirabilite [7,8,13,26]. On the other hand, several workers have shown that damage due to crystallization pressure appears to be more important than damage due to hydration pressure [27–29]. Nevertheless, at temperatures below  $32.4^\circ\text{C}$ , the damage due to crystallization pressure has always been attributed to the precipitation of mirabilite [7,8,12,13,26,27, 30]. In summary, there are contradictory data and interpretations as to why and how sodium sulfate causes damage to porous materials.

This paper is aimed to further our understanding of the crystallization and growth of sodium sulfate at room temperature ( $20^\circ\text{C}$ ) through a series of experiments under various RH conditions and on a range of supports. The results reveal some unexpected behaviors which help to explain reported inconsistencies in tests with sodium sulfate.

## 2. Materials and methods

A saturated solution of sodium sulfate (Baker, reagent grade) was prepared. The crystallization of sodium sulfate phases was observed by means of optical microscopy (Leitz, Laborlux 12 Pol), letting a solution drop evaporate on a glass slide in an environmentally controlled chamber at various RH conditions (12%, 30%, 40%, 50%, 60%). The temperature was kept constant at  $20 \pm 1^\circ\text{C}$ . In order to confirm that no temperature variation took place during the crystallization of the salts (due to the illumination system of the microscope or the heat of crystallization), the temperature was monitored continuously by using a thermocouple adhered to the bottom of the glass thin section, just beneath the drop. The precipitated phases were analyzed using X-ray diffraction (XRD, Siemens D-5000). In situ experiments on crystallization of sodium sulfate from a solution drop were also performed in the XRD chamber at controlled temperature and RH ( $20^\circ\text{C}$  and 40% RH).

High-magnification in situ analysis of the dynamics of sodium sulfate crystallization was performed using an environmental scanning electron microscope (ESEM, ElectroScan model E-3). Condensation and evaporation of water on a salt sample were obtained by modifying the temperature and pressure inside the ESEM chamber, according to the methodology described by Doehne and Stulik [32] and Messier and Vitale [33]. Images were recorded digitally. The

ESEM was also used to observe crystals precipitated on a glass slide at various RH conditions.

Sodium sulfate crystals on spall surfaces taken from porous material blocks (oolitic limestone from Monks Park, UK) deteriorated by partial immersion in sodium sulfate solutions (modified RILEM/PEN25 test) were also studied for comparative purposes using the ESEM (for details, see Refs. [34–36]).

### 3. Results

At RH values >40%, precipitation of sodium sulfate upon evaporation of a solution drop placed onto a glass slide resulted initially in the crystallization of prismatic, elongated mirabilite crystals, followed by their dehydration and transformation into microscopic thenardite crystals which were not identifiable by optical microscopy. Note that all experiments were performed at an RH less than 71%. At RH values <40%, at the drop edge or other random location within the drop, small amounts of idiomorphic thenardite crystals precipitated directly from the solution. Fig. 2a illustrates the morphology of these crystals. Thenardite tended to grow as tiny, elongated needles (phase III) grouped as dendrites. At different points within the dendritic thenardite aggregates, other large, bulky thenardite crystals were formed (bipyramidal prism of phase V). In a few cases, crystallization experiments performed at very low RH conditions (below 15%) resulted mostly in prismatic or rhombohedral bulky aggregates of phase V thenardite crystals with a small amount of phase III aggregates, and no trace of mirabilite (Fig. 2b).

The XRD analyses of the products formed following the evaporation of saturated sodium sulfate solution drops placed on a glass slide within the XRD chamber, at controlled temperature and RH (20°C and 40%, respectively), resulted in either simultaneous precipitation of mirabilite plus thenardite, or precipitation of thenardite alone. In the latter case, both phases III and V were identified (Fig. 3).

The ESEM analysis of crystals precipitated on glass slides, as well as those precipitated in situ, within the ESEM chamber at controlled temperature and pressure offered a new, high magnification picture of this crystallization process. Fig. 4a shows the morphology of the thenardite aggregates precipitated at controlled RH and temperature on glass slides. None of these morphologies corresponds to the thenardite crystals observed after dehydration of mirabilite (Fig. 4b and c). In most experiments (15°C and ~25% RH, as typical environmental conditions in the ESEM chamber), the precipitation of sodium sulfate in the ESEM resulted in the direct formation of mirabilite, followed by dehydration and crystallization of thenardite crystals which pseudomorphically replace the mirabilite with masses of micron-sized crystals (Fig. 4c). Precipitation of thenardite crystals was observed in isolated areas of the ESEM samples, such as fractures and rough portions of the aluminum sample holder (Fig. 4d). These crystals were identified as thenardite because no dehydration following precipitation took place.

The crystallization of thenardite took place in the ESEM chamber following dissolution of thenardite crystals at 15°C and 10 Torr of pressure, corresponding to a RH value of ~80% [33], followed by precipitation of sodium sulfate (both mirabilite and thenardite phases) when the pressure at the ESEM chamber was reduced to 3 Torr at 15°C, corresponding to ~25% RH. A few seconds after crystallization, mirabilite dehydration occurred. No hydration was observed when thenardite crystals were in contact with the solution. Instead, dissolution of thenardite occurred, followed by precipitation of mirabilite and thenardite.

A number of earlier experiments on salt crystallization were performed by partially immersing a porous limestone block in 300 cm<sup>3</sup> saturated sodium sulfate solution placed in a glass beaker and sealed with melted paraffin wax. Capillary rise of the solution through the stone pore system took place, followed by solution evaporation and salt crystallization at constant temperature (20°C). Environmental conditions (RH and temperature), salt crystal morphologies, and stone damage evolution were monitored continuously by means

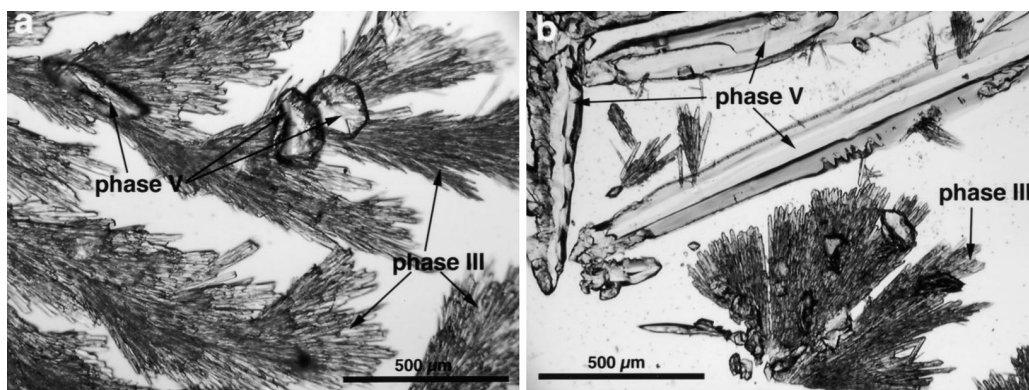


Fig. 2. Micrograph of thenardite crystals. (a) Precipitated at 20°C and low RH conditions (>40%); the needles are phase III and the prisms are phase V crystals [37]. (b) Large phase V bipyramidal prisms precipitated at 20°C and 13% RH. Small amounts of phase III needles are also present.

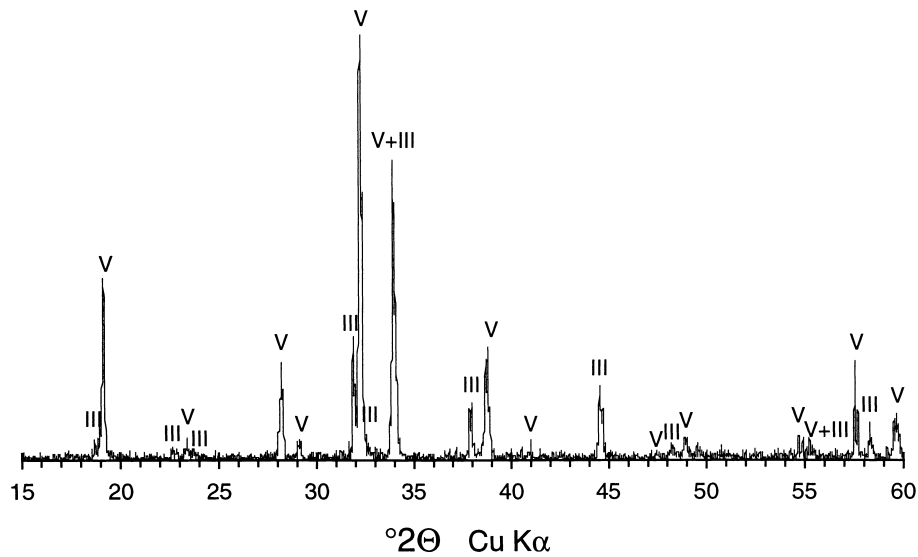


Fig. 3. The XRD pattern of thenardite (phases III and V) precipitated directly from solution at 20°C and RH < 40%.

of time lapse video microscopy [35]. Massive formation of mirabilite whisker-like crystals on the surface of the stone occurred at RH values above 60% [35,36]. These conditions were characterized by reduced damage, the stone block total weight loss being 7.1 wt.%. However, at RH values of ~40%, negligible mirabilite efflorescence was observed and

progressive millimeter-scale surface spalling resulted in substantial stone surface recession and 21.4 wt.% total weight loss [36]. ESEM analysis of scales that fell off the decayed stone faces in the experiment performed at 40% RH revealed the presence of a large number of micron- to submicron-sized thenardite crystals (Fig. 5). It is unlikely

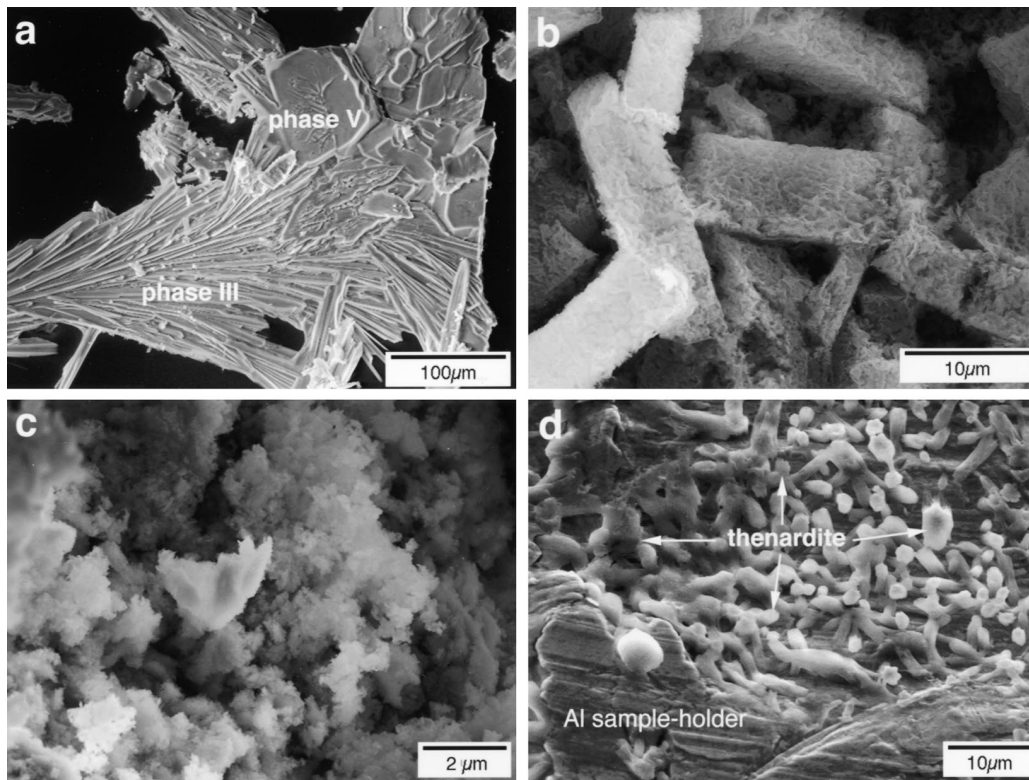


Fig. 4. Sodium sulfate ESEM micrographs. (a) Thenardite crystals precipitated on glass slides. (b) Thenardite aggregates formed after dehydration of pre-existing mirabilite crystals (ESEM dynamic study). (c) Detail of thenardite crystals formed after dehydration of mirabilite. (d) Thenardite crystals precipitated directly from solution on the Al sample holder in the ESEM.

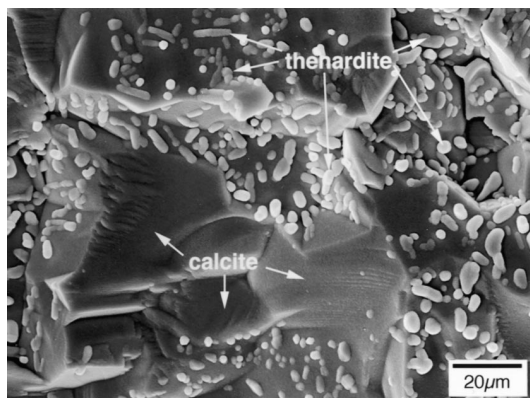


Fig. 5. Thenardite on the underside of a decayed limestone spall fragment. Note the similarity of these crystals with the thenardite crystals precipitated in the ESEM chamber (Fig. 4d).

that these crystals formed by dehydration of previously precipitated mirabilite crystals since textural evidence of this process is normally preserved (i.e., polycrystalline thenardite aggregates after mirabilite). These small, anhedral crystals similar in shape and dimensions to the thenardite crystals are observed directly precipitating in the ESEM (Fig. 4d). Thenardite on the limestone spall fragments is typically present in planar micropores (pores with radius  $< 1 \mu\text{m}$ ) adjacent to fractured calcite crystals (Fig. 5). No mirabilite crystals were observed in the latter samples.

These experimental results suggest that most of the damage to the limestone in the salt crystallization experiment carried out at 40% RH conditions was due to the crystallization of thenardite at temperatures below  $32.4^\circ\text{C}$  (the mirabilite–thenardite transition point) and at low RH. In these conditions, the solution evaporation rate was  $7.5 \text{ cm}^3/\text{day}$ , while at 60% RH it was only  $5.6 \text{ cm}^3/\text{day}$ . The higher evaporation rate conditions resulted in the crystallization of subfluorescence (i.e., crystals formed inside the stone pores). In these conditions, the evaporation front was located some distance (typically at 1–3 mm) from the stone surface, and up to 3-mm-thick scales were formed. At low evaporation rate conditions, the solution evaporation front was normally located at the stone surface, resulting in mirabilite efflorescence (i.e., whiskers) growth and reduced damage.

#### 4. Discussion

Researchers have routinely used sodium sulfate solutions to develop accelerated decay tests to simulate or reproduce decay conditions and damage to natural stone, concrete, or other building materials in a wide variety of environments [26–29,31,38–41]. Sodium sulfate is typically selected for two reasons: first, it is very common in a wide range of locations and environments [30], and second, it is extremely destructive [7,27,30,42–44]. Cooke [30] concluded that sodium sulfate is so damaging mainly because it undergoes a high degree of volume change when hydrated. However,

even in experiments where hydration did not take place, the resulting damage was impressive [27,29,34–36]. According to data from Winkler and Wilhelm [8], the precipitation of the anhydrous phase, thenardite, could generate larger crystallization pressures and thus more damage than the crystallization of mirabilite. This assumption was confirmed experimentally by Sperling and Cooke [27]. They observed that at low humidity conditions (i.e., fast evaporation) and temperatures leading to thenardite crystallization, damage was always more significant (in a range of stone types) than at conditions leading to mirabilite crystallization [27]. Nonetheless, Winkler and Singer [9] as well as Sperling and Cooke [27], in agreement with data established at the beginning of the century for the  $\text{Na}_2\text{SO}_4\text{--H}_2\text{O}$  system [18], reported that thenardite will only precipitate at temperatures above  $32.4^\circ\text{C}$ . Our experimental results indicate the contrary: under normal (i.e., non-equilibrium) conditions, thenardite precipitates directly from solution (at low RH; i.e., high evaporation rate conditions) and creates significant damage at lower temperatures ( $20^\circ\text{C}$ ). Additionally, ESEM data show that upon wetting, thenardite does not hydrate to form mirabilite. Instead, thenardite is dissolved, followed by mirabilite as well as thenardite crystallization. Thus, it seems that part of the damage attributed in the literature to crystallization pressure of mirabilite may, in fact, have been caused by crystallization pressure of the thenardite. On the other hand, our experimental results indicate that most of the damage attributed to the hydration pressure of mirabilite may, in fact, corresponds to crystallization pressure of mirabilite (crystallizing alone or together with thenardite). This implies that careful attention should be paid to identify which phase is crystallizing when salt crystallization tests are performed.

It seems that heterogeneous nucleation of thenardite over a defect (roughness, dust, crystals surface defects, fractures, scratches, etc.) on a glass slide, on an aluminum sample holder, or over calcite minerals in a limestone pore, is one of the main factors controlling or inducing thenardite precipitation and growth at temperatures below  $32.4^\circ\text{C}$ . In fact, in natural systems, far-from-equilibrium, heterogeneous nucleation on impurities, micropores, fractures, or crystal defects is thermodynamically more stable and plausible than homogeneous nucleation [45]. Many of the substrates where damage due to sodium sulfate is found have high internal surface areas. Moreover, materials with a large fraction of micropores (large surface area) have long been noted as being more susceptible to sodium sulfate damage than macroporous materials [42].

According to Tardy and Nahon [46], the water activity,  $a_{\text{H}_2\text{O}}$ , in a pore is related to the pore radius,  $r$ , by the following equation (Eq. (1)):

$$\log a_{\text{H}_2\text{O}} = \frac{-9.21 \times 10^{-4}}{2r}. \quad (1)$$

The inverse relation between the water activity and the pore radius implies that in small pores or capillaries, formation of

anhydrous phases will be promoted [47], while hydrated phases will form in the larger pores. This explains why on smooth glass slides small amounts of thenardite precipitate directly from the solution, and in the case of the ESEM experiments these crystals tended to be located in small pores or fractures on the aluminum sample holder. However, thenardite massively formed in the micropores of the oolitic limestone ( $\sim 0.25 \mu\text{m}$  average pore radius, according to Ref. [36]) where significant damage occurred.

It seems that a high degree of supersaturation is a prerequisite for thenardite precipitation at  $20^\circ\text{C}$ . Crystallization experiments carried out onto a glass slide at high RH resulted in slow solution evaporation and massive, prismatic, equilibrium morphology mirabilite crystals. Equilibrium morphologies of crystals are indicative of low supersaturation ratios [36,48]. Decreasing RH and faster evaporation conditions resulted in thenardite crystallization, thenardite crystals either being equilibrium-shaped prisms (phase V) or non-equilibrium needles (phase III). The latter morphology corresponds to slightly higher supersaturation ratios. In the aluminum sample holder in the ESEM chamber where fast evaporation occurred, thenardite formed in pores or fractures as crystals with far-from-equilibrium morphologies, indicative of higher supersaturation ratios [36,48]. In our crystallization tests using a porous support, high RH conditions resulted in slow evaporation and massive mirabilite whisker growth. Soluble salts whiskers are formed at low supersaturation ratios [38]. On the other hand, low RH conditions resulted in fast evaporation and thenardite nucleation and growth as anhedral, needle-shaped or bow tie aggregates. These morphologies correspond to crystals formed at very high supersaturation ratios [48].

Crystallization of thenardite at high supersaturation ratios resulted in significant damage to the porous stone. According to the formula for salt crystallization pressure developed by Correns [49], the crystallization pressure,  $P$ , is directly proportional to the supersaturation ratio (Eq. (2)):

$$P = \frac{RT}{V_s} \ln \frac{C}{C_s}, \quad (2)$$

where  $V_s$  is the molar volume of solid salt,  $C$  is the concentration of the saline solution,  $C_s$  is the solution saturation concentration at temperature  $T$ , and  $R$  is the gas constant. Winkler and Singer [9] calculated crystallization pressures for mirabilite and thenardite and observed that for the same supersaturation ratios, thenardite could generate higher pressures than mirabilite (almost one order of magnitude higher), thus being potentially more destructive [27]. However, it is not known how much supersaturation can be sustained before mirabilite or thenardite crystallizes in a porous material. Therefore, the absolute crystallization pressure of each salt in a real case scenario (i.e., in a stone or concrete pore) is very difficult to evaluate (if not impossible). By analyzing the crystal morphology and determining how much it varies from the equilibrium shape, it is possible to give a qualitative estimate of the supersaturation ratio during

nucleation. Hence, the crystallization pressure reached in a pore can be estimated. Crystal morphology data point to higher supersaturation ratios, and therefore higher crystallization pressures in the case of thenardite if compared with mirabilite. This is consistent with the observed damage to the stone support submitted to sodium sulfate crystallization test.

The pore size of a building material is an important parameter controlling the supersaturation reached before crystallization starts. In pores of small radius ( $< 1 \mu\text{m}$ ), the pressure in the solution filling the pore can differ considerably from the corresponding pressure of the bulk solution due to the Laplace effect of curvature [50]. This pressure reduction results in increased supersaturation of the solution filling the pore when the molar volume of the condensed phase (solid) is greater than the molar volume of the solute in solution, as it is the case of sodium sulfate. When nucleation starts, the nucleation rate will be inversely proportional to the pore radius. Therefore, in a porous system, a solution of sodium sulfate will sustain supersaturation ratios higher than the critical supersaturation ratio it can sustain outside the pores, and when crystallization starts, a large number of crystals will form. This is consistent with the large amount of thenardite crystals with far-from-equilibrium morphologies observed in the porous stone with extensive damage. It also explains why far-from-equilibrium thenardite crystal morphologies are more common in the stone pores and cracks on the ESEM aluminum sample holder than on the smooth surface of the glass slide. Since thenardite tends to crystallize in small pores at high supersaturation ratios, pressures enough to overcome the tensile strength of the porous support develop, resulting in building material breakdown. On the other hand, mirabilite crystallization either in larger pores as equilibrium-shaped crystals or on the surface of the porous material as whiskers formed at low supersaturation conditions [38] results in little damage.

In natural field conditions, periodic crystallization/dissolution and/or hydration/dehydration processes are typical with alternating wetting/drying cycles due to rain or condensation. Sodium sulfate crystals in a porous material may precipitate originally either as thenardite, or as mirabilite plus thenardite mixtures, depending on the environmental conditions and the porous system characteristics. Later on, mirabilite may undergo dehydration, resulting in the formation of thenardite. As water accesses the system again, thenardite may dissolve, forming a saturated solution following evaporation, and finally precipitating alone or together with mirabilite. In any case, only crystallization pressure (no hydration pressure) will be responsible for building material damage.

## 5. Conclusions

From the results presented and discussed above, the following conclusions can be drawn. (1) The system,

$\text{Na}_2\text{SO}_4\text{-H}_2\text{O}$ , as defined at the beginning of the century (equilibrium conditions), is inconsistent with the actual (real world) crystallization of thenardite from solution at temperatures below  $32.4^\circ\text{C}$  (the thenardite–mirabilite transition point). We found that the classic definition of the system, while being accurate for homogeneous (equilibrium) crystallization, does not explain our results. In natural, heterogeneous (non-equilibrium) systems, heterogeneous nucleation of thenardite is promoted at temperatures below  $32.4^\circ\text{C}$  at low RH, fast solution evaporation, and high supersaturation ratios. (2) Most sodium sulfate crystallization tests attribute almost all damage to sodium sulfate hydration within a porous material (hydration pressure). Our experimental results suggest that this view should be reconsidered. Our results show that only crystallization pressure occurs. Furthermore, thenardite crystallization may be responsible for much of the damage. Thus, careful attention should be paid to identify which phenomenon (crystallization vs. hydration) and which phase are responsible for the damage, and under which environmental conditions the test is carried out. (3) In situ ESEM observation of crystallization events is a useful tool for the dynamic study of salt crystallization and growth. Using an ESEM, micron-scale thenardite and mirabilite were observed growing in situ at high magnification at temperatures below  $32.4^\circ\text{C}$  ( $15^\circ\text{C}$  and  $\text{RH} < 30\%$ ). No mirabilite hydration was observed. Instead, dissolution of pre-existing thenardite crystals, followed by crystallization of mirabilite plus thenardite, occurred. The classical attribution of damage due to hydration of thenardite to form mirabilite is not consistent with our results. (4) Non-equilibrium thenardite morphologies developed in situ in the ESEM under rapid crystallization conditions (high supersaturation) are similar to those present on micropore surfaces (spall samples) from deteriorated limestone where crystallization of sodium sulfate took place at  $20^\circ\text{C}$  and low RH ( $< 40\%$ ). (5) Observed thenardite morphologies precipitated at  $20^\circ\text{C}$  and low RH reflect high supersaturation ratios, which result in high crystallization pressures and significant damage to porous materials. (6) Heterogeneous nucleation of thenardite appears to explain the formation of this phase at temperatures below the transition point of mirabilite–thenardite. The reduction of the energy necessary for the formation of stable thenardite nuclei seems to be large enough to prevent the formation of mirabilite. For this to occur, high supersaturation ratios appear to be a prerequisite (low RH and fast evaporation of the saline solution, or rapid cooling). Additionally, a significant water activity reduction in the smaller pores and capillaries of the porous support induces the formation of non-hydrated phases (thenardite). (7) The presence of very small pores (micropores) in the tested oolitic limestone induces high supersaturation ratios of the sodium sulfate solution before crystallization occurs. High supersaturation ratios result in high sodium sulfate crystallization pressure and significant damage to the porous support. This effect may explain why

microporous materials are more susceptible to sodium sulfate crystallization damage than macroporous ones.

Few data are currently available on the influence of the support (rock, existing crystals, etc.) on soluble salt crystallization and damage. The study and evaluation of the supersaturation ratio reached by a saline solution before heterogeneous nucleation and growth of sodium sulfate crystals as well as other soluble salts occur in a pore, needs to be encouraged to better understand this important process with direct implications in the fields of crystal growth, geomorphology, the conservation of cultural heritage, and civil engineering.

### Acknowledgments

We are indebted to K. Elert, W.S. Ginell, E. Hansen, B. McCarthy, and A. Arnold for discussing and critically reviewing the original manuscript. The comments and suggestions of an anonymous referee have contributed to the improvement of this paper. This research was developed and performed as part of the “Preservation of Porous Calcareous Stone” project undertaken by the Getty Conservation Institute. Financial support has been provided also by the CYCIT (Spanish Government) under contract no. PB96-1445.

### References

- [1] A.S. Goudie, H. Viles, *Salt Weathering Hazards*, Wiley, Chichester, 1997.
- [2] G.A. Novak, A.A. Colville, Efflorescent minerals assemblages associated with cracked and degraded residential concrete foundations in Southern California, *Cem Concr Res* 19 (1989) 1–6.
- [3] T. Ritchie, Study of efflorescence produced on ceramic wicks by masonry mortars, *J Am Ceram Soc* 38 (1955) 362–366.
- [4] M.A. Halliwell, N.J. Crammond, in: C. Sjoström (Ed.), *Durability of Building Materials and Components*, E&FN Spon, London, 1996, pp. 235–244.
- [5] D.A. St. John, An unusual case of ground water sulphate attack on concrete, *Cem Concr Res* 12 (1982) 633–639.
- [6] S. Chatterji, A.D. Jensen, Efflorescence and breakdown of building materials, *Nord Concr Res* 8 (1989) 56–61.
- [7] I.S. Evans, Salt crystallization and rock weathering: a review, *Rev Geomorphol Dyn* 19 (1970) 153–177.
- [8] E.M. Winkler, E.J. Wilhelm, Salt burst by hydration pressures in architectural stone in urban atmosphere, *Geol Soc Am Bull* 81 (1970) 567–572.
- [9] E.M. Winkler, P.C. Singer, Crystallization pressure of salt in stone and concrete, *Geol Soc Am Bull* 83 (1972) 3509–3514.
- [10] ASTM C 88-90, Standard test method for soundness of aggregate by use of sodium sulfate or magnesium sulfate, *Annu Book ASTM Stand* 4.2 (1997) 37–42.
- [11] RILEM PEM/25, Essais recommandées pour l’altération des pierres et évaluer l’efficacité des méthodes de traitement, *Mater Constr* 17 (1980) 216–220.
- [12] C.A. Price, The use of sodium sulphate crystallisation test for determining the weathering resistance of untreated stone, in: UNESCO/RILEM International Symposium on Deterioration and Protection of Stone Monuments Vol. 3.6, Reilure, Paris, 1978, pp. 1–23.

- [13] H. Marschner, Application of salt crystallization test to impregnated stone, in: UNESCO/RILEM International Symposium on Deterioration and Protection of Stone Monuments Vol. 3.4, Reilure, Paris, 1978, pp. 1–15.
- [14] W. Sheftick, Na<sub>2</sub>SO<sub>4</sub> soundness test evaluation, *Cem Concr Aggregates* 11 (1989) 73–79.
- [15] B. Hunt, There's no alternative, *Stone Ind* (1994) 37–39.
- [16] O. Knacke, R. Von Erdberg, The crystallization pressure of sodium sulfate decahydrate, *Ber Bunsen-Ges Phys Chem* 79 (1975) 653–657.
- [17] O. Braitsch, *Salt Deposits: Their Origin and Composition*, Springer, New York, 1971.
- [18] H. Hartley, B.M. Jones, G.A. Hutchinson, The spontaneous crystallisation of sodium sulphate solutions, *J Chem Soc* 93 (1908) 825–833.
- [19] W.F. Linke, *Solubilities, Inorganic and Metal Organic Compounds: A Compilation of Solubility Data From the Periodical Literature*, Van Nostrand-Reinhold, Princeton, 1958.
- [20] H. Stephen, T. Stephen, *Solubilities of inorganic compounds, Binary Systems Vol. 1*, Macmillan, New York, 1933.
- [21] A. Arnold, Behavior of some soluble salts in stone monuments, in: T.H. Skoulikidis (Ed.), *2nd International Symposium on the Deterioration of Building Stones*, National Technical University, Athens, 1976, pp. 27–36.
- [22] Gmelin, *Handbuch der Anorganischen Chemie*, Verlag Chemie, Weinheim, 1927.
- [23] W. Eysel, Crystal chemistry of the system Na<sub>2</sub>SO<sub>4</sub>–K<sub>2</sub>SO<sub>4</sub>–K<sub>2</sub>CrO<sub>4</sub>–Na<sub>2</sub>CrO<sub>4</sub> and the glaserite phase, *Am Mineral* 58 (1973) 736–747.
- [24] H. Naruse, K. Tanaka, H. Morikawa, F. Marumo, Structure of Na<sub>2</sub>SO<sub>4</sub> (I) at 693 K, *Acta Crystallogr, Sect B* 43 (1987) 143–146.
- [25] E. Doehne, In situ dynamics of sodium sulfate hydration and dehydration in stone pores, in: V. Fassina, H. Ott, F. Zezza (Eds.), *Proceedings of 3rd International Congress on the Conservation of Monuments in the Mediterranean Basin*, Graffo, Venice, 1994, pp. 143–150.
- [26] A.S. Goudie, Sodium sulfate weathering and the disintegration of the Mohenjo-Daro, Pakistan, *Earth Surf Process* 2 (1977) 75–86.
- [27] C.H.B. Sperling, R.U. Cooke, Laboratory simulation of rock weathering by salt crystallization and hydration processes in hot, arid environments, *Earth Surf Processes Landforms* 10 (1985) 541–555.
- [28] F.J.P.M. Kwaad, Experiments on the granular disintegration of granite by salt action, *Fys Geogr en Bodemkundig Lab* 16 (1970) 67–80 (Amsterdam University).
- [29] B.D. Fahey, A comparative laboratory study of salt crystallization and salt hydration as potential weathering agents in deserts, *Geogr Ann Ser A: Phys Geogr* 68 (1986) 107–111.
- [30] R.U. Cooke, Salt weathering in deserts, *Proc Geol Assoc London* 92 1981, pp. 1–16.
- [31] K. Pye, C.H.B. Sperling, Experimental investigation of silt formation by static breakage processes: the effect of temperature, moisture and salts on quartz dune salt and granitic regolith, *Sedimentology* 30 (1983) 49–62.
- [32] E. Doehne, D. Stulik, Application of the environmental scanning electron microscope to conservation science, *Scanning Microsc* 4 (1990) 275–286.
- [33] P. Messier, T. Vitale, Cracking in albumen photographs — an ESEM investigation, *Microsc Res Tech* 25 (1993) 374–383.
- [34] C. Rodriguez-Navarro, E. Doehne, E. Sebastian, W.S. Ginell, Salt growth in capillary and porous media, in: E.M. Sebastian, E. Valverde, U. Zezza (Eds.), *3rd International Congress on Restoration of Building and Architectural Heritage*, Arco Impresores, Granada, 1996, pp. 509–514.
- [35] C. Rodriguez-Navarro, E. Doehne, Time lapse video and ESEM: integrated tools for understanding processes in situ, *Am Lab* 31 (1999) 28–35.
- [36] C. Rodriguez-Navarro, E. Doehne, Salt weathering: influence of evaporation rate, supersaturation and crystallization pattern, *Earth Surf Processes Landforms* 24 (1999) 191–209.
- [37] V. Amirthaligam, M.D. Karkhanavala, U.R.K. Rao, Topotaxial phase change in Na<sub>2</sub>SO<sub>4</sub>, *Acta Crystallogr, Sect A* 33 (1977) 522–523.
- [38] K. Zehnder, A. Arnold, Crystal growth in salt efflorescence, *J Cryst Growth* 97 (1989) 513–521.
- [39] J.C. Doornkamp, H.A.M. Ibrahim, Salt weathering, *Prog Phys Geogr* 14 (1990) 335–348.
- [40] A. La Iglesia, V. González, V. López-Acevedo, C. Viedma, Salt crystallization in porous construction materials: I. Estimation of crystallization pressure, *J Cryst Growth* 177 (1997) 111–118.
- [41] G.W. Scherer, Crystallization in pores, *Cem Concr Res* 29 (1999) 1347–1358.
- [42] R.J. Schaffer, *The weathering of natural building stones*, DSIR, Building Research Station Special Report No. 18, Stationary Office, London, 1932, p. 34.
- [43] A.E. Charola, J. Weber, The hydration–dehydration mechanism of sodium sulfate, in: J.D. Rodrigues, F. Henriquez, J.T. Jeremias (Eds.), *7th International Congress on Deterioration and Conservation of Stone*, Laboratorio Nacional de Engenharia Civil, Lisbon, 1992, pp. 581–590.
- [44] D.J. McMahon, P. Sandberg, K. Folliard, P.K. Mehta, Deterioration mechanisms of sodium sulfate, in: J.D. Rodrigues, F. Henriquez, J.T. Jeremias (Eds.), *7th International Congress on Deterioration and Conservation of Stone*, Laboratorio Nacional de Engenharia Civil, Lisbon, 1992, pp. 705–714.
- [45] W.A. Tiller, *The Science of Crystallization: Microscopic Interfacial Phenomena*, Cambridge Univ. Press, Cambridge, 1991.
- [46] Y. Tardy, D. Nahon, Geochemistry of laterites, stability of Al-goethite, Al-hematite and Fe<sup>3+</sup>-kaolinite in bauxites and ferricretes: an approach to the mechanisms of concretion formation. *Am J Sci* 285 (1985) 865–903.
- [47] A. La Iglesia, M.A. Garcia, S. Ordoñez, The physicochemical weathering of monumental dolostones, granites and limestones; dimension stones of the Cathedral of Toledo (Spain), *Sci Total Environ* 152 (1994) 179–188.
- [48] I. Sunagawa, Characteristics of crystal growth in nature as seen from the morphology of mineral crystals, *Bull Miner* 104 (1981) 81–87.
- [49] C.W. Correns, Growth and dissolution of crystals under linear pressure, *Discuss Faraday Soc* 5 (1949) 267–271.
- [50] D. Kashchiev, G.M. van Rosmalen, Effect of pressure on nucleation in bulk solutions and solutions in pores and droplets, *J Colloid Interface Sci* 169 (1995) 214–219.